ELSEVIER

Journal of Power Sources 74 (1998) 255–258

JOURNAL OF POWER SOURCES

Short communication

Electrocatalytic activity of spinel-type oxides $LiMn_{2-X}Co_XO_4$ with large specific surface areas for metal–air battery

Neng Li *, Xiaoming Yan, Wanjing Zhang, Bingxiong Lin

Institute of Physical Chemistry, Peking University, Beijing 100871, China

Received 5 February 1998; accepted 8 February 1998

Abstract

A series of spinel-type oxides $LiMn_{2-X}Co_XO_4$ ($X = 1.0, 1.2, 1.4, 1.6$) are synthesized by an improved amorphous citric precursor (ACP) method. Their specific surface areas are measured by the Brunauer-Emmet-Teller (BET) method, and their particle agglomerates are studied by scanning electron microscopy (SEM). Their electrocatalytic performances are characterized by the polarization curves of gas-diffusion electrodes that employ the oxides. The activity decreases with increasing X values.

Keywords: $LiMn_{2-X}Co_XO_4$; Metal–air battery; Electrocatalysis; Cathode material

1. Introduction

The metal–air battery is an attractive power source due to its high specific energy [1], but it is not used widely because of the lack of an ideal cathode electrocatalyst. Such an electrocatalyst must possess high activity, low price, and be stable in alkaline solution [2,3]. Moreover, electrocatalysts with large specific surface areas are necessary in order to obtain high activity [3–5]. Some spinel-type oxides [6–8] promise to be good cathode electrocatalysts for metal–air batteries because of their high activity for oxygen evolution in alkaline solution [4]. Lithium manganese spinel-type oxides has been widely examined as cathode materials for lithium batteries and rechargeable lithium-ion batteries [9,10]. In this study, a series of $LiMn_{2-X}Co_XO_4$ with large specific surface area have been synthesized by an improved amorphous citric precursor method (IACP), and their electrocatalytic performance has been elucidated in gas-diffusion oxygen electrodes.

2. Experimental

Spinel-type oxides, $LiMn_{2-X}Co_XO_4$ ($X = 1.0, 1.2, 1.4, 1.6$), were synthesized by IACP. The solutions of nitrates of constituent ions and citric acid were mixed, and then a certain amount of carbon black was added in order to prevent agglomeration of the particles of the oxides. The mixture was decomposed at 200°C for 1 h, calcined at 360°C in air for 4 h, and then cooled to ambient temperature. No carbon remained in the samples. The same series of complex oxides were also synthesized by the traditional ACP [11] method in order to compare the difference between the two methods. The specific surface areas of the oxides were measured by the Brunauer–Emmet–Taylor (BET) method (N_2 adsorption). The average grain size of each oxide was obtained by X-ray diffraction (XRD) analysis (Rikagu, D/max − r_A Cu Kα, 40 kV, 150 mA). The particle agglomerate structures of the samples were investigated by means of scanning electron microscopy (SEM) (Amray 1910 FE), and transmission electron microscopy (TEM) (JEM-200cx). The constant k_m of the H_2O_2 decomposition reaction catalyzed by the oxides was measured in 7 M KOH solution at 20.0°C (error is less than 5%) [12]. Gas-diffusion oxygen electrodes were fabricated by using the procedure of Shimizu et al. [3]. The reaction layer consisted of 25 wt.% oxide catalyst (1.5 mg cm^{-2}),

* Corresponding author.

60 wt.% carbon black and 15 wt.% PTFE. The gas-diffusion layer consisted of ethyne black (70 wt.%), PTFE (30 wt.%) and an embedded nickel mesh (current-collector). The total thickness of the electrode was about 0.6 mm. The half-cell was that developed by Li et al. [12]. The polarization curves, referred to a Hg/HgO electrode, were measured in 7 M KOH at 20.0°C under an oxygen flow (100 $cm^3\ min^{-1}$).

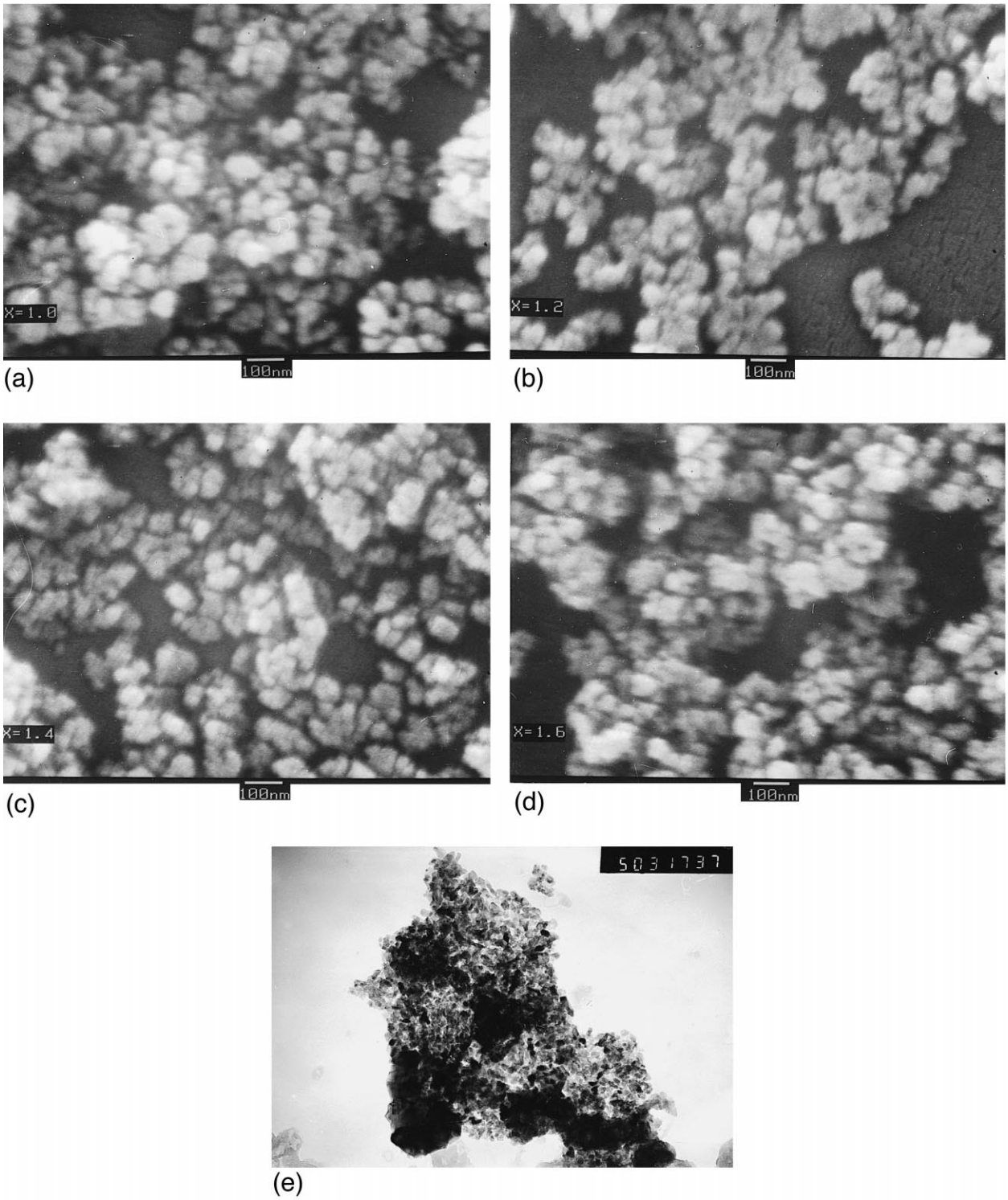

Fig. 1. Electron micrographs of spinel-type oxides. (a)–(d) SEM studies of IACP oxides; (e) TEM of ACP oxide; (a) $LiMnCoO_4$; (b) $LiMn_{0.8}Co_{1.2}O_4$; (c) $LiMn_{0.6}Co_{1.4}O_4$; (d) $LiMn_{0.4}Co_{1.6}O_4$; (e) $LiMnCoO_4$ ($\times 8 \times 10^4$).

Table 1
Average grain size ($D_{(100)}$) and specific surface area(s) of the improved amorphous citric precursor (IACP) oxides, together with their respective H_2O_2 decomposition constants

X in $LiMn_{2-X}Co_XO_4$	$X=1.0$	$X=1.2$	$X=1.4$	$X=1.6$
$D_{(100)}$ (nm)	15	18	21	21
S ($m^2\ g^{-1}$)	45.8	36.6	35.6	34.3
k_m ($10^{-3}\ s^{-1}\ g^{-1}\ m^{-2}$)	17.7	13.2	5.17	1.86
D_{cal} (nm)	28	35	36	37
ρ ($g\ cm^{-3}$)	4.67	4.69	4.70	4.71

Table 2
Average grain size ($D_{(100)}$) and specific surface area (S) of amorphous citric precursor (ACP) oxides, together with their respective H_2O_2 decomposition constants

X in $LiMn_{2-X}Co_XO_4$	$X=1.0$	$X=1.2$	$X=1.4$	$X=1.6$
$D_{(100)}$ (nm)	28	27	25	20
S ($m^2\ g^{-1}$)	21.6	21.3	21.4	24.7
k_m ($10^{-3}\ s^{-1}\ g^{-1}\ m^{-2}$)	0.708	0.447	0.404	0.270
D_{cal} (nm)	63	64	65	55

3. Results and discussion

The average grain size of the IACP oxides increases with increasing X value, meanwhile while the specific surface area decreases (Table 1). The reverse trends are found with oxides obtained by the traditional ACP method (Table 2). Moreover, the surface areas of the former oxides are much larger than the latter. The addition of carbon black weakens the agglomerates of the oxide particles and increases the specific surface area. The microstructural features of the oxides are shown in Fig. 1. The order of particle size, though different to that measured by XRD, is $D_{1.0} < D_{1.2} < D_{1.4} < D_{1.6}$. Assuming the particles be ideal spheres or cubes, then the average particle size, D_{cal}, is related simply to the specific surface area, S, by the formula [6]: $D_{cal} = 6/S\rho$, where ρ is the theoretical density, which is obtained by XRD analysis in this paper. The calculated results, listed in Table 1, are so similar to those obtained by SEM analysis that it is concluded that the space among the particles is sufficiently large for nitrogen molecules to enter and be absorbed. An agglomerate of

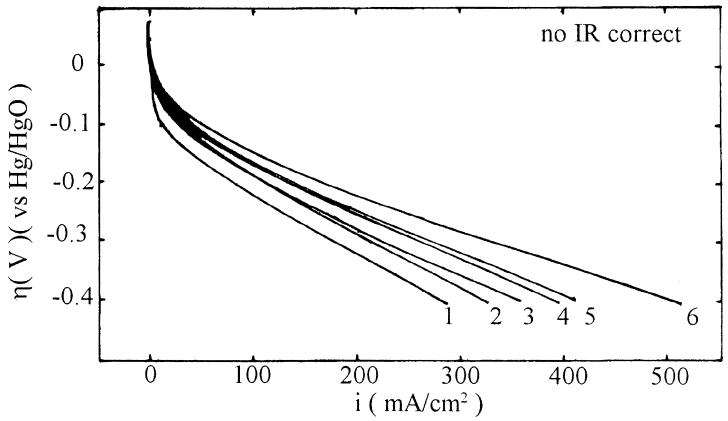

Fig. 2. Cathodic polarization curves (for oxygen reduction) of gas-diffusion carbon electrodes loaded with $LiMn_{2-X}Co_XO_4$ with different X values: (1) carbon, (2) $X=1.0$ (in air), (3) $X=1.6$, (4) $X=1.4$, (5) $X=1.2$, (6) $X=1.0$.

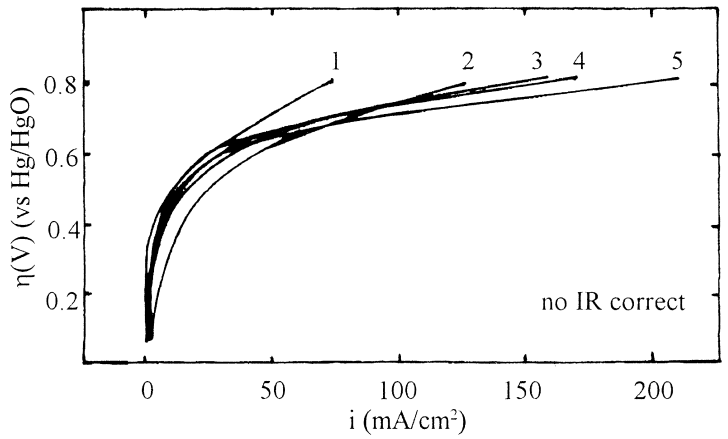

Fig. 3. Anodic polarization curves (for oxygen evolution) of gas-diffusion carbon electrodes loaded with $LiMn_{2-X}Co_XO_4$ with different X values: (1) carbon, (2) $X=1.6$, (3) $X=1.4$, (4) $X=1.2$, (5) $X=1.0$.

$LiMnCoO_4$ (ACP) particles is shown in Fig. 1e. The size of the agglomerated particles is about 24 nm, and is similar to that measured by XRD. The size is also similar to that of $LiMnCoO_4$ (IACP) particles shown in Fig. 1a. The particles agglomerate so closely however, that the specific surface area is much smaller than that of particles obtained by the IACP method.

The polarization curves of various working electrodes are given in Figs. 2 and 3. All the electrodes loaded with catalysts perform better than the carbon electrode. The cathode performance is sensitive to the partial pressure of oxygen, P_{O_2}. The order of the performance of both cathodes and anodes is $1.0 > 1.2 > 1.4 > 1.6$, which is determined by an electronic factor and a microstructural feature. In Table 1, the specific surface area, S, represents the microstructural feature, while k_m of the H_2O_2 decomposition reaction normalized by the specific surface area represents the electronic factor because a large k_m generally means a high electrocatalytic activity. The trend in the values of both these parameters vs. X is the same, so the same order appears in the electrode performance.

It should also be noticed that k_m catalyzed by the IACP oxides is much larger than that catalyzed by ACP oxides. Thus, addition of carbon black not only weakens the particle agglomerates but also changes the structural parameters of the complex oxide. Oxides, $LiMn_{2-X}Co_XO_4$ ($X < 1.0$), which are expected to possess higher catalytic activity, have been successfully synthesized under different conditions, and their properties will be reported in a later article.

References

[1] M.H. Frank, J.S. Mark, Proc. 10th Annu. Battery Conf. Appl. Adv., 1995.
[2] L. Swetter, J. Giner, J. Power Sources 22 (1988) 399.
[3] Y. Shimizu, K. Uemura, H. Matsuda, N. Miura, N. Yamazoe, J. Electrochem. Soc. 137 (1990) 3430.
[4] H.M. Cota, T. Katan, M. Chin, F.J. Schoenweis, Nature 4951 (1964) 1281.
[5] S.K. Tiwari, S.P. Singh, R.N. Singh, J. Electrochem. Soc. 143 (1996) 1505.
[6] J.R. Goldstein, A.C.C. Tseung, J. Catal. 32 (1974) 452.
[7] R.N. Singh, J.-F. Koening, G. Poillerat, P. Chartier, J. Electrochem. Soc. 137 (1990) 1408.
[8] B. Marsan, N. Fradette, G. Beaudoin, J. Electrochem. Soc. 139 (1992) 1889.
[9] M.M. Thackeray, L.A. De Picciotto, A. De Kock, P.J. Johnson, V.A. Nicholas, K.T. Adendorff, J. Power Sources 21 (1987) 1.
[10] J. Desilverstro, O. Haas, J. Electrochem. Soc. 137 (1990) 5c.
[11] C. Marcilly, P. Courty, B. Delmon, J. Am. Ceramic Soc. 53 (1970) 56.
[12] Q. Li, G. Xiao, H.A. Hjuler, R.W. Berg, N.J. Bjerrum, J. Electrochem. Soc. 141 (1994) 3114.